Journal of the European Ceramic Society **17** (1997) 1403–1414

PII: S0955-2219(96)00244-0
0955-2219/97/$17.00

Highly Ordered Pyrolytic BN Obtained by LPCVD

F. Rebillat,[a] A. Guette,[a] R. Naslain[a] & C. Robin Brosse[b]

[a]Laboratoire des Composites Thermostructuraux, UMR 47, CNRS-SEP-UB1, 3 allée de la Boëtie, 33600 Pessac, France
[b]SEP-Le Haillan, BP, 37 33165 Saint-Médard-en-Jalles, France

(Received 8 August 1996; revised version received 20 November 1996; accepted 25 November 1996)

Abstract

The chemical and physical properties of boron nitride are improved as soon as its crystallisation degree in the hexagonal modification is high, the structure becoming somewhat similar to that of graphite. Under such conditions, it can be used (instead of pyrocarbon) as an interphase in ceramic matrix composites. Unfortunately, under commonly used CVD/CVI conditions, BN layers display only a poor turbostratic texture. Furthermore, when BN is deposited from the BF_3–NH_3 system, the fibrous reinforcement can be chemically damaged. A wide range of BN coatings and especially a three-dimensionally ordered hex-BN have been deposited by LPCVD at relatively low temperature. Structural evolution in BN coatings was related to change in chemical rate control regimes. Finally, a compromise between conditions yielding anisotropic coatings and conditions resulting in low degradation of the fibres has been worked out. © 1997 Elsevier Science Limited.

1 Introduction

SiC/SiC composites, as for many other fibrous ceramic matrix composites (CMCs), exhibit a high toughness, with respect to monolithic ceramics, coupled to an extended non-linear behaviour under tensile loading, when properly processed. These properties are directly related to the occurrence of various well-identified energy-dissipating mechanisms, i.e. matrix microcracking, fibre/matrix debonding and fibre sliding and pull-out. These mechanisms contribute to increase dramatically the work of fracture and resistance to crack propagation, and to avoid catastrophic failure.[1,2] However, it is now well established that the onset of these energy-dissipating mechanisms requires a low enough shear strength interface between the fibres and the matrix.[3] This requirement is usually achieved through the use of an interfacial compliant material, referred to as the interphase. So far, materials with a layered crystal structure such as carbon have been the most widely used interphases.[4]

When the debond occurs within the interphase (which supposes a strong fibre/interphase bonding), the bonding energy depends only on the intrinsic properties of the coating. Thus, the mechanical behaviour of the composites is related to that of the interphase. In a recent work, Dupel *et al.*[5] showed that the microtexture of a pyrocarbon interphase, deposited by pulsed chemical vapour deposition (PCVI), can be controlled by varying the conditions of deposition.

Boron nitride has been suggested as an alternative to anisotropic pyrocarbon in various CMCs for service at elevated temperatures in oxidizing atmospheres.[6–10] There is indeed a marked similarity between BN and carbon.[11–13] Further, BN displays an unusual combination of properties including thermal stability, corrosion resistance and mechanical properties.[14–16]

The aim of this work was to obtain adherent thin coatings of Pyro-BN by low pressure chemical vapour deposition (LPCVD) on SiC fibres with a controlled microtexture in order to achieve a range of mechanical characteristics similar to that previously reported for pyrolytic carbon interphases. Thus, a study on the degree of organization of the BN coatings as well as the evolution of the mechanical properties of coated fibres as a function of the deposition conditions was carried out. Finally, CVD conditions resulting in the deposition of anisotropic boron nitride at low temperature were worked out.

2 Experimental Procedure

Boron nitride is often poorly crystallized. Heat treatments at very high temperatures (beyond 2000°C) are required to obtain hexagonal boron nitride.[17,18] Generally, heteroatoms such as oxygen

and iron favour this crystallization.[18–20] An alternative is plasma-enhanced chemical vapour deposition, but even under such conditions dopants are still needed.[21]

A decrease of the graphitization temperature can be achieved by sintering under high pressure (> 200 MPa), but aids are still required.[20] Hexagonal BN coatings could also be obtained at lower temperatures via polymer precursor routes, but they are not stable and very sensitive to moisture.[22] However, a hexagonal BN material with a high anisotropy is required to increase the stability under oxygen or moisture until 1000°C.[18,23,24]

2.1 Apparatus

In their pioneering works, Pierson, Hannache *et al.* and Prouhet *et al.* have established the feasibility of the infiltration of a BN matrix in a fibrous preform from the gaseous BF_3–NH_3 system.[21,25,26] The choice of boron trifluoride versus boron trichloride was motivated by the higher thermodynamical stability of the former and the smaller number of side reactions and products.[26]

In the present work, the BN depositions were carried out in a hot-wall low-pressure CVD reactor. The apparatus used in this study has been described elsewhere.[21] The BF_3 and NH_3 injection nozzles are located in a hot enough zone in order to prevent the formation of complex compounds such as BF_3 NH_3 or BF_4 NH_4 (which are solid at low temperatures). The reactor is equipped with accurate temperature (818 P from Eurotherm) and total pressure (552 A from MKS Instruments) regulation. All the gas flow rates (Q_{BF3}, Q_{NH3} and Q_{Ar}) are measured with mass flowmeters (AFC 25 from ASTM).The entrance composition of the gas phase is described by the $\alpha = Q_{NH3}/Q_{BF3}$ and $\beta = Q_{Ar}/(Q_{NH3}+Q_{BF3})$ ratios. The duration of BN deposition on the fibres is 3 h. The deposition conditions were chosen in such a way that a relatively extended range of conditions (involving ΔT = 100°C, ΔP = 4 kPa, ΔQ = 40 sccm and $\Delta\alpha$ = 1·6) could be scanned with a minimum number of experiments (Table 1 and Fig. 1). The bases for the choice of these conditions were given elsewhere.[21,26]

2.2 The substrates

BN was deposited on desized Si–C–O Nicalon fibres (SiC-ex PCS Nicalon NLM 202 fibre from Nippon Carbide) produced from polycarbosilane (PCS). The fibre surface is known to be enriched in oxygen over a thickness of about 10 nm. Because of the presence of a silicon oxycarbide amorphous phase in the fibre, Nicalon fibres become unstable at 1100–1200°C.[27–29] Thus, in SiC/BN/SiC composites, a SiO_2/C dual layer, resulting from a decomposition undergone by the fibres upon processing, is always present at the fibre BN interface and constitutes the weakest bond in the interfacial sequence.[30,31]

The fibres were extracted from a bundle and the single filaments fixed straight on a graphite frame. The frames were placed in the hot zone of the CVD reactor. Occasionally, for more specific studies about the texture of BN, a few coatings were deposited on graphite, sintered α-SiC or SiO_2 planar substrates.

2.3 Characterization

The morphology of the deposit on the fibres was characterized by scanning electron microscopy (SEM) and transmission electron microscopy (TEM).[32,33]

X-Ray diffraction patterns are recorded by using D-5000 equipment from Siemens and Cu K_α radiation (λ = 1·54 Å). X-Ray diffraction was used to assess the BN crystallization state and to evidence the preferred orientations of the (002) planes against the substrate surface. Pole figures were recorded from BN films deposited on planar substrates. A pole figure is obtained by recording through a stereographic projection the intensity

Table 1. CVD conditions for BN coating and mechanical properties obtained from tensile tests

References	T *(°C)*	P *(kPa)*	Flows Q_{NH3} + Q_{BF3}	α= Q_{NH3}/Q_{BF3}	σ^r(0·5) *(MPa)*	*Weibull modulus* m	*Young modulus (GPa)*	*Thickness of BN* (μm)	ε^r (%)	*Coating roughness*	*Coating adhesion*
1	–	–	+	+	2650	6·1	200	0·1	1·26	small	strong
2	–	+	+	–	2300	6	175	0·24	1·3	big	weak
3	+	–	–	+	2015	6·1	173	0·18	1·14	medium	strong
4	–	+	–	+	2304	8	182	0·17	1·28	small	strong
5	+	+	+	+	986	6·3	107	2·8	0·98	big	weak
6	+	–	+	–	2382	6·9	181	0·35	1·28	small	strong
7	+	+	–	–	2000	6·7	183	0·25	1·11	small	medium
8	–	–	–	–	2305	6·2	197	0·07	1·15	small	strong
9	0	0	0	0	2136	9·3	171	0·5	1·21	small	weak

with – : Lower limit in the studied domain. with T_0, P_0, α_0, Q_0.
0 : Middle condition with T_0 + 50°C, P_0 + 2 kPa, α_0 + 0·8, Q_0 + 20 sccm.
+ : Upper limit in the studied domain with T_0 + 100°C, P_0 + 4 kPa, α_0 + 1·6, Q_0 + 40 sccm.

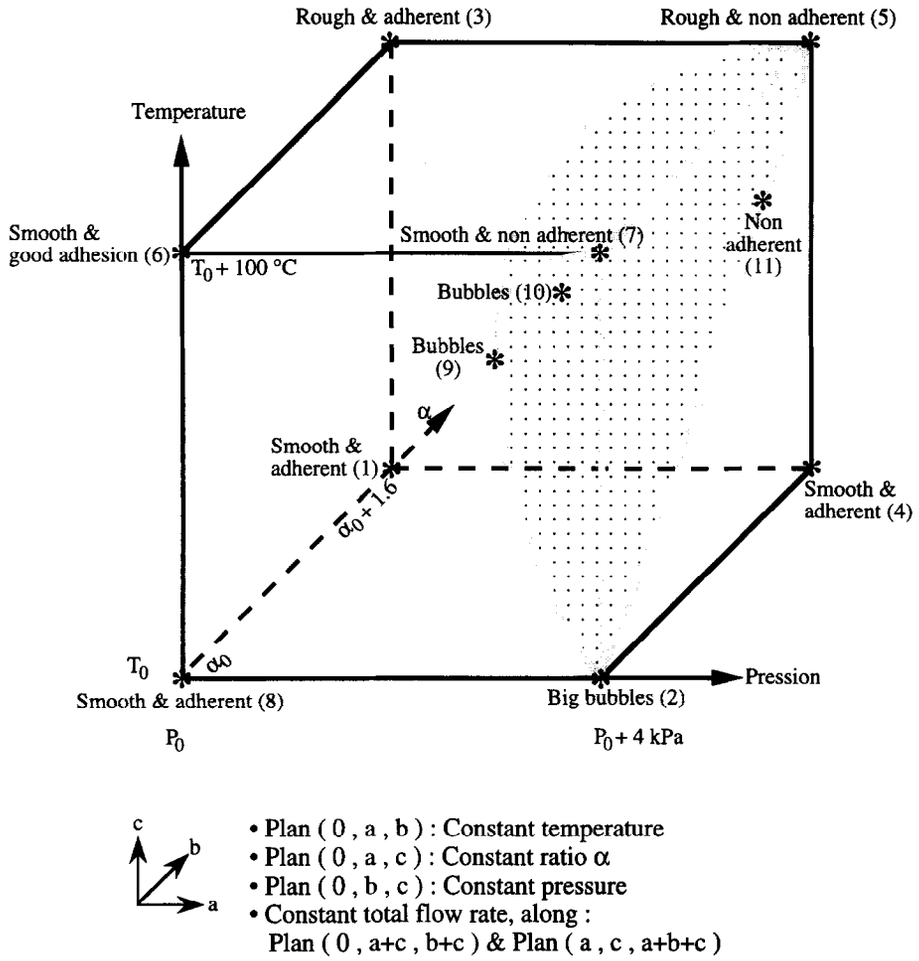

Fig. 1. Schematic showing the studied (temperature, pressure, composition, flow rate) domain of BN deposition, (the references of the experimental CVD conditions are shown in parenthesis.

diffracted by a (hkl) plane when the sample is tilted in all possible orientations in space. The points of iso-intensity are linked by contour lines and the pole figure corresponds to a three-dimensional representation of the data (using TEX-AT software from SOCABIM). The point with the maximal intensity gives the direction in which the maximum of the (hkl) planes are stacked with a certain order between each other.

The coated fibres were also subjected to single fibre tensile tests. The corrosion of the fibres during the process leads to the modification of the population of the surface defects with an alteration of the failure properties. The mechanical data have been analysed according to a two-parameters Weibull distribution (probabilistic approach of failure).

2.4 Transverse fibre cross-sections for transmission electron microscopy

The interfacial fibre coating zone and the BN interphase anisotropy perpendicular to the fibre surface were studied from transverse cross-sections. A possible method initially used for the preparation of carbon fibre sections for TEM[34] involves setting the fibres in a pre-set block of resin and thinning the sample by Ar^+ ion etching. However, the resin thins down more quickly than the fibre because of the differential etching rate and the fibres fall down and are lost.

A new procedure[35] for making transverse thin sections from our samples was required. A ceramic cement (supplied by AREMCO, (ref 569 or 603)) consisting of a slurry of sub-micronic alumina powder in a polymer was preferred to embed the fibres. This cement displays after hardening a very small residual porosity ≤ 1% and does not require any treatment at high temperatures. The successive steps of the procedure can be summarized as follows: (i) embedding the fibres, (ii) cutting thin slices with a diamond saw, polishing mechanically, and (iii) etching by argon ions.

3 Results

3.1 Morphology of BN deposits

Within the studied domain of CVD conditions (Table 1 and Fig. 1), when the four different parameters evolve toward the highest values of temperature, pressure, reactive gas flow rate (Q_{BF3} + Q_{NH3}) and α ratio (β = constant) (Fig. 1 and

Table 2), only narrow variations of conditions give neat changes of morphology (Figs 2 and 3). To complete the data in this limited part, more experiments (conditions 10,11) were explored between the middle (conditions 9) and the extreme (conditions 5) points corresponding to the highest variations of ΔT, ΔP, $\Delta\alpha$ and ΔQ (Figs 1 and 3 and Table 2).

Generally, in this range of processing conditions, the fibres are perfectly embedded in the BN deposit, as observed by SEM. After processing, no cracking due to a relaxation of high residual thermally induced stresses is observed along the fibres. In general, the observation by SEM of the BN layers shows a rather smooth surface with small grain sizes (Fig. 2). Such a structure is often related to slow growth rates ($< 0{\cdot}15\ \mu m\ h^{-1}$). Further, the appearance of 'waves' along the coating surface is related to the presence of voids at the fibre/BN interface (Figs 2(b), 2(c) and 3).

Particularly, for the highest values of processing parameters, i.e. from the conditions 9 to the extreme conditions 5 (through 10 and 11), chemical results exhibit a progressive evolution (Table 2): (i) the growth rate of the BN coating increases from 0·17

Table 2. Mechanical characteristics of coated Nicalon fibers with an evolutive textured BN (duration of processing: 3 h)

References conditions	σ^r (0·5) *(MPa)*	*Weibull modulus* (m)	*Young modulus (GPa)*	ε^r (%)	*Thickness of BN coating* (μm)	*Growth rate of BN coatings* ($\mu m\ h^{-1}$)
SiC ex-PCS fiber	2300	4·3	207	1·1	0	0
9	2136	9·3	171	1·21	0·5	0·17
10	1660	9·4	153	1·14	0·84	0·28
11	1420	7·5	143	0·98	1·38	0·46
5	986	6·3	107	0·98	2·8	0·93

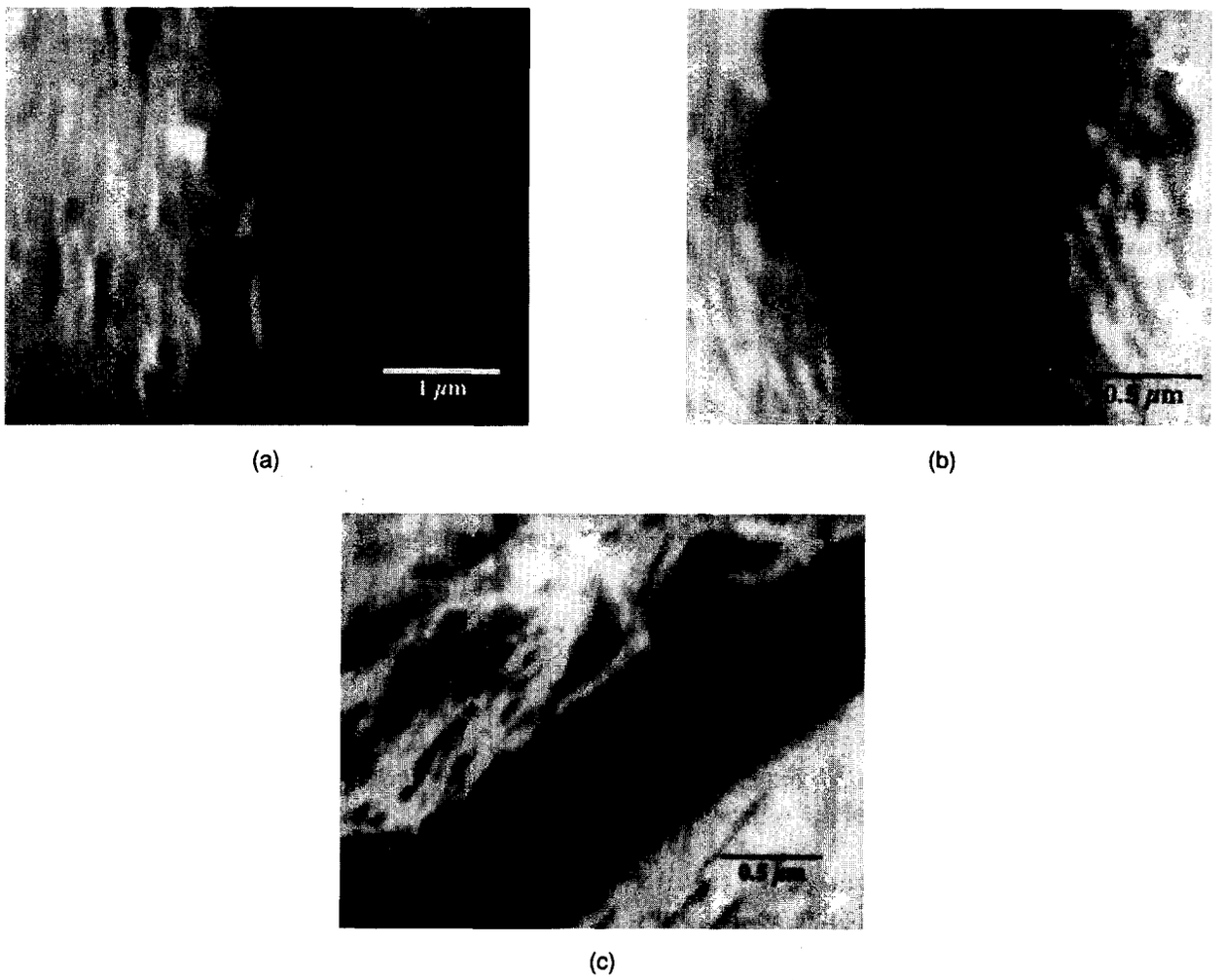

Fig. 2. Characterization by scanning electron microscopy of the roughness and the adhesion of BN coating on Nicalon fibers: (a) smooth coating with a good adhesion (conditions 1), (b) coating with discontinuities of adherence, i.e. bubbles (conditions 9), and (c) smooth coating but with a poor adhesion (conditions 7).

to 0·93 μm h^{-1}, (ii) the observation of coating surfaces reveals the presence of grains with more and more sharp edges, (Fig. 3) and (iii) the BN coating seems less and less bonded to the fibres as suggested by scanning electron microscopy.

For the conditions 5 corresponding to the extreme point, the scanning electron microscopy shows a deposit with faceted grains as columns with sharp edges around flat-topped surfaces (Figs 3(c) and 4(a)). The diameters of these columns are estimated to be about 1 μm in size (measured at the surface of a coating 2·8 μm in thickness) (Fig. 4(a)). Finally, the shape of the crystals reveals that the BN coatings become more and more organized in the hexagonal structure (Fig. 4(b)) as opposed to the relatively smooth surfaces related to isotropic phases.[21,30,31]

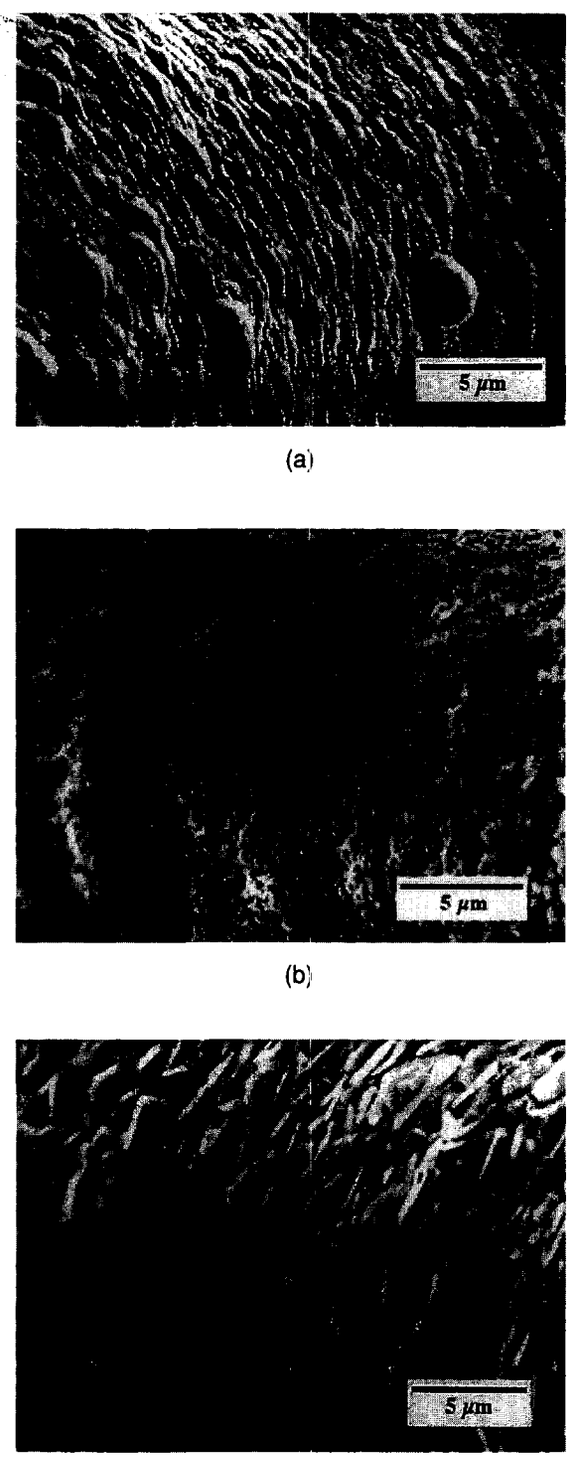

Fig. 3. Characterization by SEM of the crystallisation state of BN coatings on Nicalon fibers as a function of processing conditions: (a) conditions 10, (b) conditions 11, and (c) conditions 5.

3.2 XRD analyses

The BN coating are often too thin and not sufficiently crystallized to give a XRD pattern that can be separated from that of SiC fibre substrates. Only the four last-mentioned BN deposits are considered here (conditions 9, 10, 11 and 5).

The XRD patterns of these BN layers show a rapid evolution of the structure when the deposition conditions are changed from the middle (9) to the limit (5) points (Fig. 4(b)). This feature can be easily related to the structural evolution (Fig. 3). The high order in the BN coating processed in the conditions 5 is confirmed by its interreticular distances very close to the theoretical

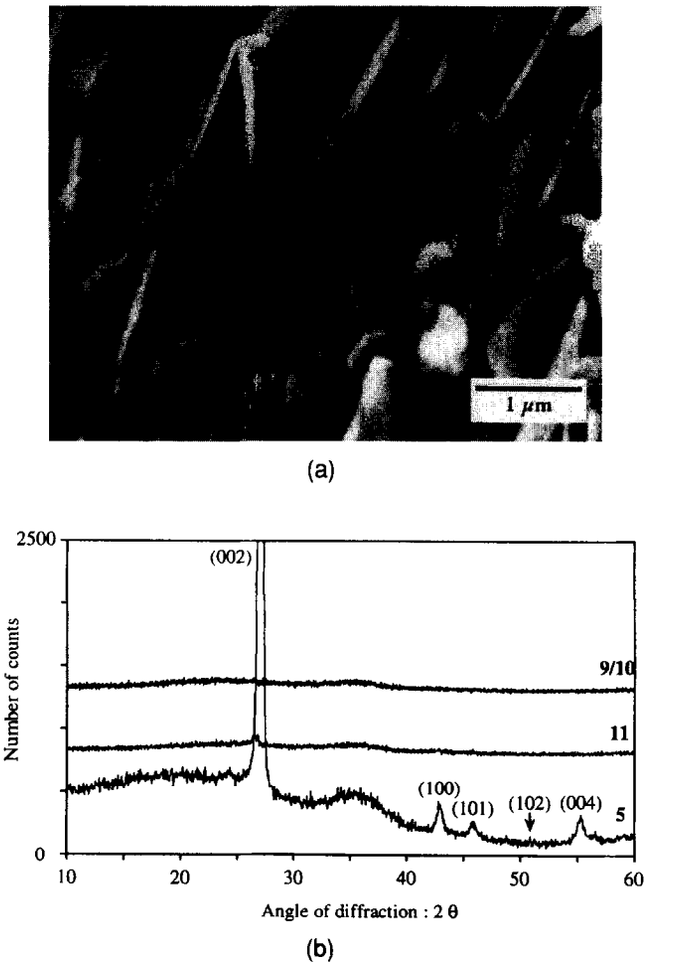

Fig. 4. High degree of crystallization of a BN coating deposited by CVD on Nicalon fibers : (a) high magnification SEM image of the well-crystallized BN coating (5), and (b) XRD diagrams showing the evolution of the degree of organization in BN coating for the processing conditions: 9, 10, 11 and 5.

values, with 3·34 and 1·67 for the (002) and (004) planes against respectively 3·328 and 1·664 from the ASTM file (Reference: 34–421).

An XRD study was carried out on the most organized BN coating (deposited on flat substrates) by using the method of pole figures (Fig. 5). The (002) pole figure shows a pronounced preferential direction of growth perpendicular to the substrate surface. The width of the peak is related to some disorder in the stacking of (002) planes. In a disordered structure, when the sample is tilted, many planes remain in the conditions of diffraction, and the peak is very wide. In Fig. 5, the experimental peak is relatively narrow showing a pronounced preferential order of growth along a direction perpendicular to the (002) planes (e.g. parallel to the fibre surface). The peak corresponding to the (004) planes is linked up to the order along the $\vec{c}$ axis, or the growth direction, and its intensity decreases when the order disappears. This latter peak is well resolved as shown in Fig. 4(b) (BN processed in the conditions 5).

3.3 TEM characterization

The TEM analyses confirm the trends evidenced from both the SEM observation of the BN deposits (Fig. 3) and the order in BN structures from the XRD studies (Fig. 4(b)).

3.3.1 Hexagonal BN processed in the CVD/CV conditions 5

As seen in Fig. 6, the BN deposited in the conditions 5 grows with a columnar texture. In each column, all the (002) planes are parallel to each other and to the fibre surface. In a grain, the presence of extended bands is related to defects in the stacking of the (002) planes (Fig. 7). Between the columns, the (002) planes are less extended

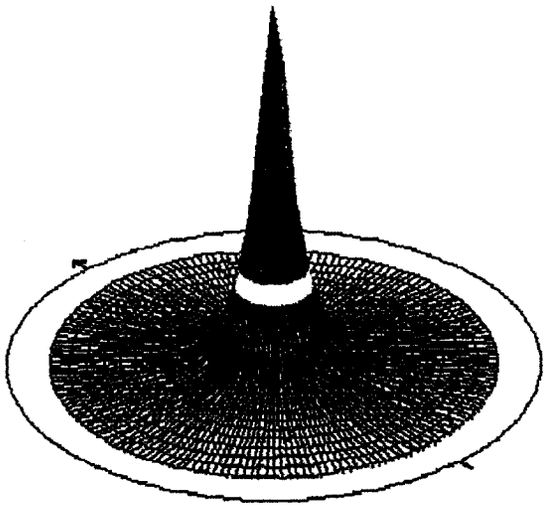

(a)

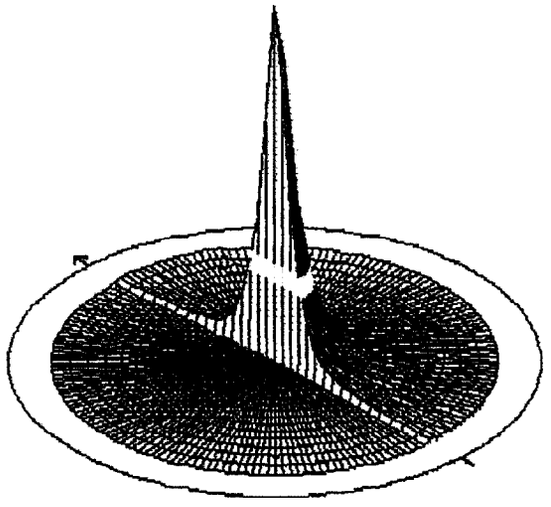

(b)

Fig. 5. XRD pole figure from the (002) planes of a BN coating processed by CVD/CVI in the conditions 5 : (a) symmetry and (b) width of the peak.

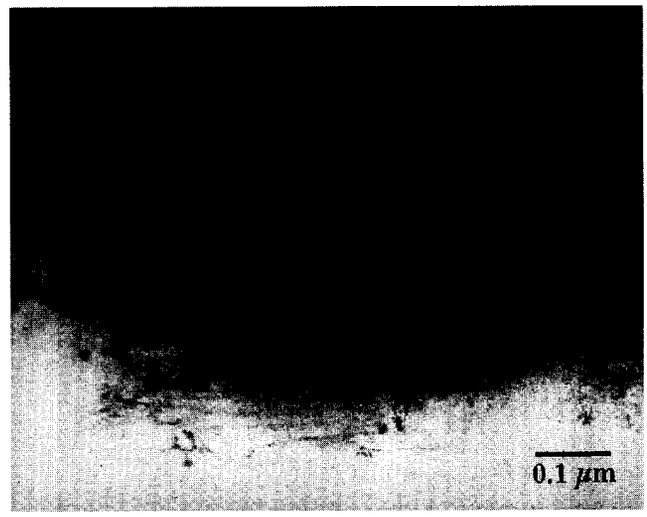

(a)

(b)

Fig. 6. Crystallized BN coating in the hexagonal structure: (a) shape of a crystal, and (b) 002 lattice fringe image and SAD pattern (in the inset).

and a disorder can exist (Fig. 7). This phenomenon is also observed at the beginning of the growth of the BN coating (close to the SiC ex-PCS fibre surfaces on which it is placed).

PEELS analysis gives a qualitative composition of the deposit. The pattern (Fig. 8) shows that the BN layer contains only very small quantities of carbon and oxygen.

3.3.2. Evolution of BN textures toward a hexagonal BN

When the deposition conditions evolve from conditions 5 toward the middle conditions 9, the grain boundaries disappear quickly (Figs 6(a), 9, 10). The extension of the (002) planes become also smaller and they are not as well as organized parallel to each other. In addition, the stacking defects are less extended, and finally order is only observed on very short distances. (002) stacks are made by a smaller number of planes, and they are more and more bent (Fig. 9).

For the coating processed in conditions 9 and 10, the size of stacks of the (002) planes is almost unchanged, but a preferential orientation is observed parallel to the fibre surface for the last conditions (Fig. 9). On the other hand, in the conditions 11, stackings are much larger and very well-organized zones, probably small crystals, appear (Fig. 10). Furthermore, the selected area diffraction (SAD) images evidence the progressive ordering of atomic planes. Successively with the increase of the processing parameters (P, T, α, Q), these images are formed by: diffuse rings (for the conditions 9), a beginning of arcs (conditions 10), only short arcs with points (conditions 11), and only points (conditions 5) (Fig. 11).

Further, despite a very rough surface aspect observed by SEM for the well-crystallized coating, the TEM analysis shows a very dense deposit without porosity. In contrast, as soon as bending of the (002) plane is observed, nano-porosities are present, mainly in the middle of bent stackings.

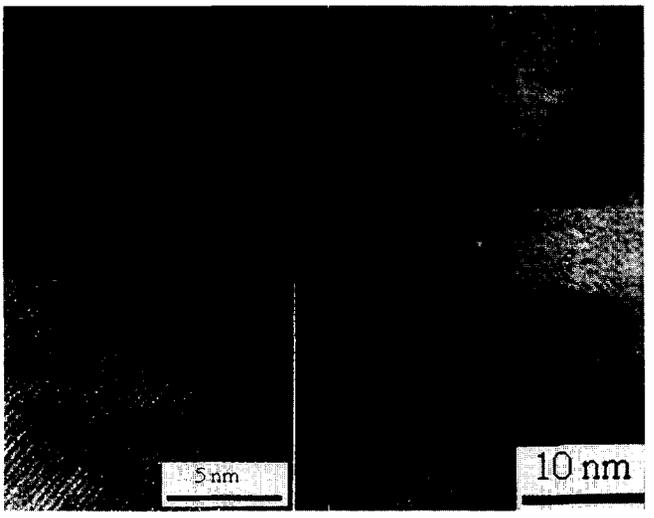

Fig. 7. 002 lattice fringe HR-TEM image of the hexagonal BN (conditions 5) coating showing defects in a crystal and, in the inset, (002) planes at a higher magnification.

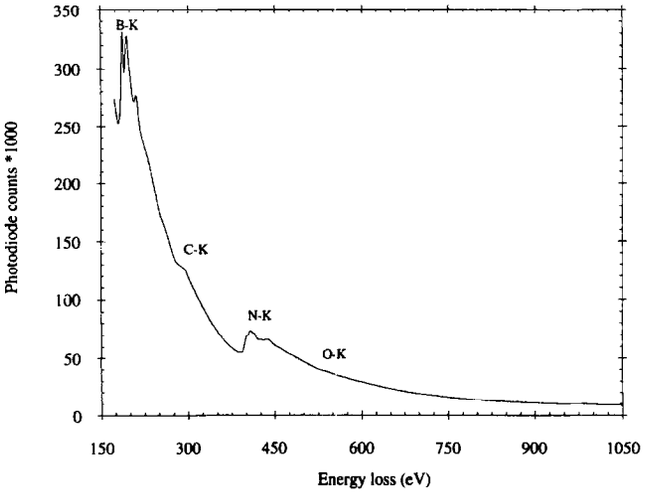

Fig. 8. PEELS spectrum of hex-boron nitride deposited on SiC Nicalon fibers (conditions 5).

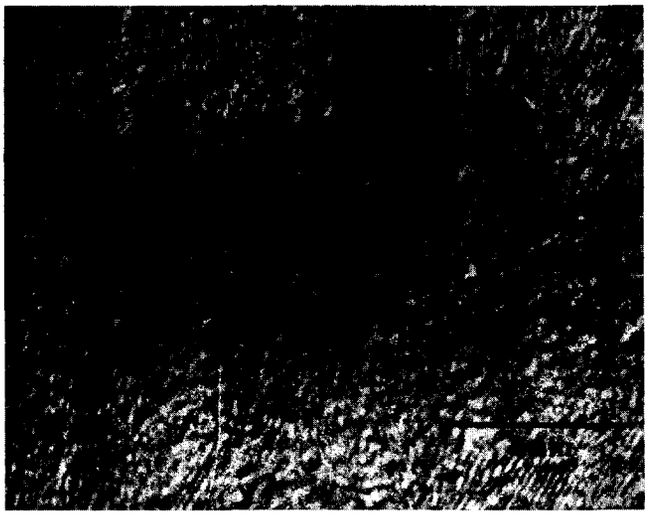

(a)

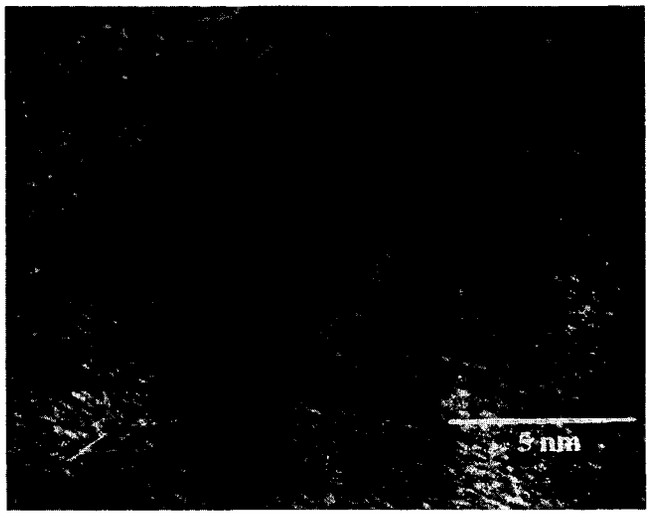

(b)

Fig. 9. TEM observation of textures in BN coatings with the increase of the processing parameters (T, P, a, Q): (a) conditions 9 and (b) conditions 10.

3.4 Mechanical characterization

The gauge length for the single fibre tensile tests is 25 mm. The following mechanical characteristics are noted: the failure strain (ε^r), the Young's modulus (E), the failure stress at 50% chance of survival ($\sigma^R_{(0\cdot5)}$), and the Weibull modulus (m). The mechanical data for the SiC ex-PCS Nicalon fibres are: $\sigma^R_{(0\cdot5)}$ = 2300 MPa, m = 4·1, ε^R = 1·1% and E = 207 GPa.[36]

With the exception of conditions 5, the failure stress ($\sigma^R_{(0\cdot5)}$) of the fibres remains almost unchanged, despite the presence of coatings (Table 1 and Fig. 12). The failure stress was calculated with the assumption that the load is uniform across the section of the coated fibre. The adherence of coatings on the fibres was evaluated by SEM observation of the failure surfaces. Owing to the shock wave at failure, a debond can be initiated at the fibre/BN interface when the BN is weakly bonded to the fibre. From these observations, across the cube schematizing the studied domain (Fig. 1), an approximate surface between the deposition conditions yielding BN coatings weakly bonded to the fibres can be drawn. Mainly, as already mentioned for the highest values of (P, T, Q, α), BN coating seems less and less bonded to the fibres,

By comparing the mechanical data of coated fibres (Fig. 12), adhesion of BN and surface morphology of coatings, some points related to development conditions are highlighted:

(i) the highest failure stress (2650 MPa) is obtained for the conditions 1 considered as the least aggressive against the fibres,[36] i.e. the lowest temperature and total pressure and the highest flow rates and α coefficient (low partial pressure of BF_3) (Table 1);

(ii) the medium conditions, conditions 9, seem to result in a very uniform mild attack of the fibre surface (failure stress smaller than that of the initial fibres), but the Weibull coefficient displays the highest value (m = 9·3) despite a weak fibre/coating adhesion (Tables 1 and 2, Fig. 2(b));

(iii) the best compromise seems to be the conditions 4 (with the highest pressure and α coefficient and the lowest temperature and flow rates) that yield a BN deposit with: (a) no damage to the fibres ($\sigma^R_{(0\cdot5)}$ = 2300 MPa), (b) a high increase of the Weibull parameter (m = 8), and (c) a coating remaining bonded to fibres with a small surface roughness;

(iv) for the conditions 5, the coated fibres displaying a non-linear stress-strain curve similar to those of composites, the failure stresses calculated by taking into account the whole section of coated fibres cannot be directly compared to those of the other coated fibres since only the fibre supports the load at ultimate failure (however, it is reported in Fig. 12);

(v) between the conditions 9 and the extreme conditions 5 (through 10, 11), the failure stress decreases catastrophically from about 2150 MPa to 1000 MPa, and the Weibull shape parameter follows a similar trend (Table 2) (their Weibull distributions should be placed in Fig. 12 between those for conditions 9 and 5; not here for the clarity of the figure).

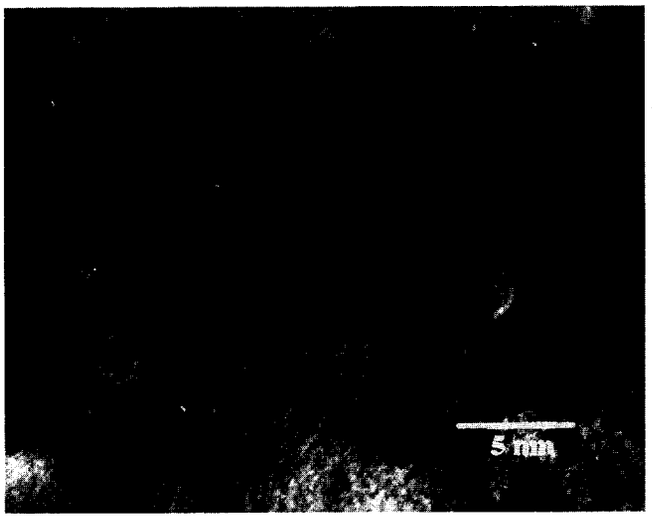

(a)

(b)

Fig. 10. TEM image of a BN coating prepared in the conditions 11: (a) crystal growth, and (b) details on the organization of the (002) planes.

4 Discussion

4.1 Quantification of the order in the BN structure

The XRD patterns can be indexed on the basis of a hexagonal unit cell. The most significant evidence

marking the onset of the three-dimensional ordering is the resolution of the broad (10) reflection into the (100) and (101) reflections, with the sharpening of the (002) reflection and the appearance of the (004) and (102) reflections.[18,20,38,39] In only more highly ordered samples, the (103) reflection appears.[18]

In our case, for the best crystallized BN coating (conditions 5), we observed a good resolution of the (100) and (101) as well as the (102) and (004) reflections. Finally, all these characteristics describe a structure with a high degree of three-dimensional order.

4.2 TEM analysis

The different steps in the process of graphitization of carbon as a function of the heat treatment temperature (HTT) reported by Oberlin *et al.*[33] can be used here to describe BN textures: (i) misoriented

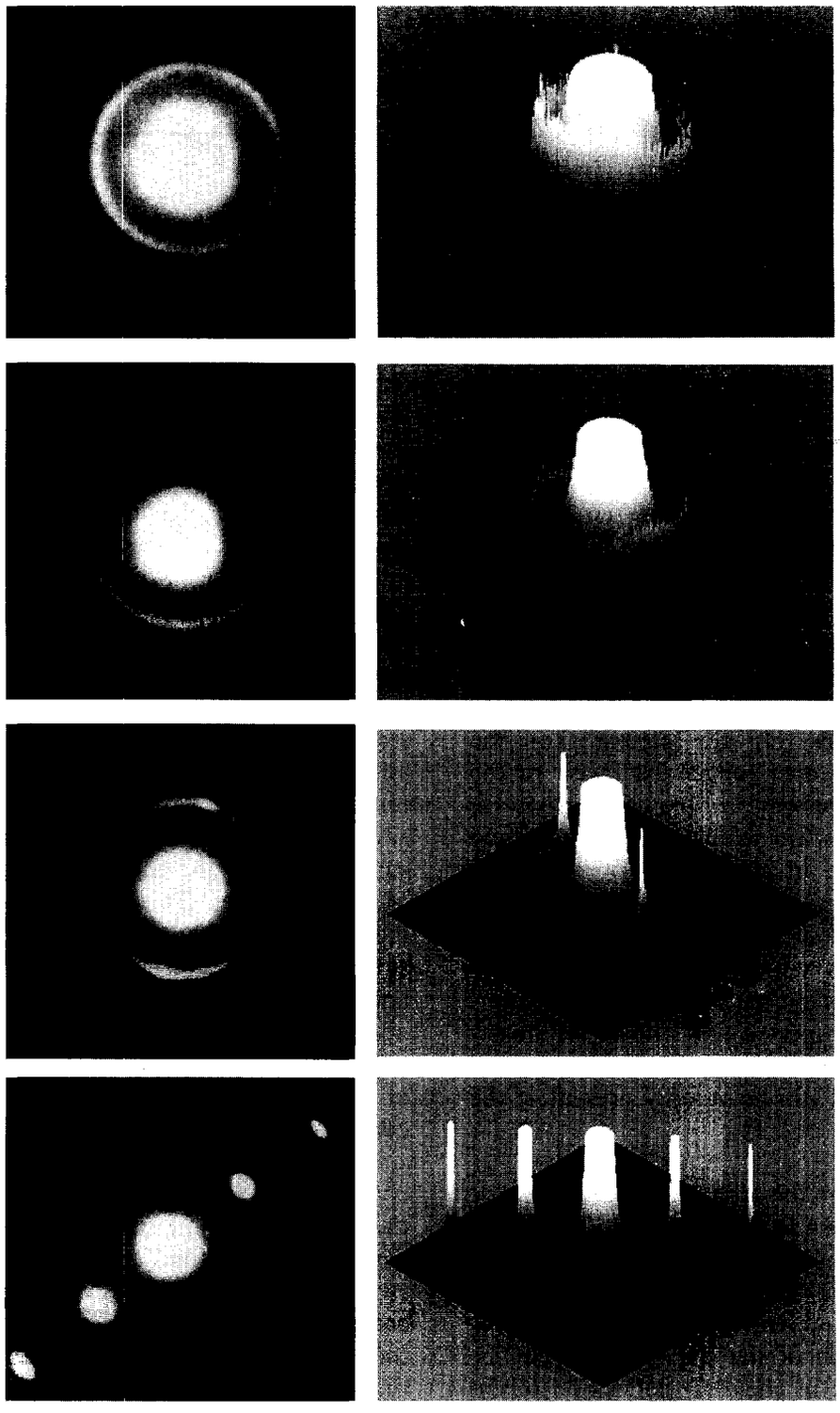

Fig. 11. SAD images and 3D perspectives of progressively more ordered BN coatings, processed in CVD/CVI conditions involving an increase of the parameters (P, T, a, Q).

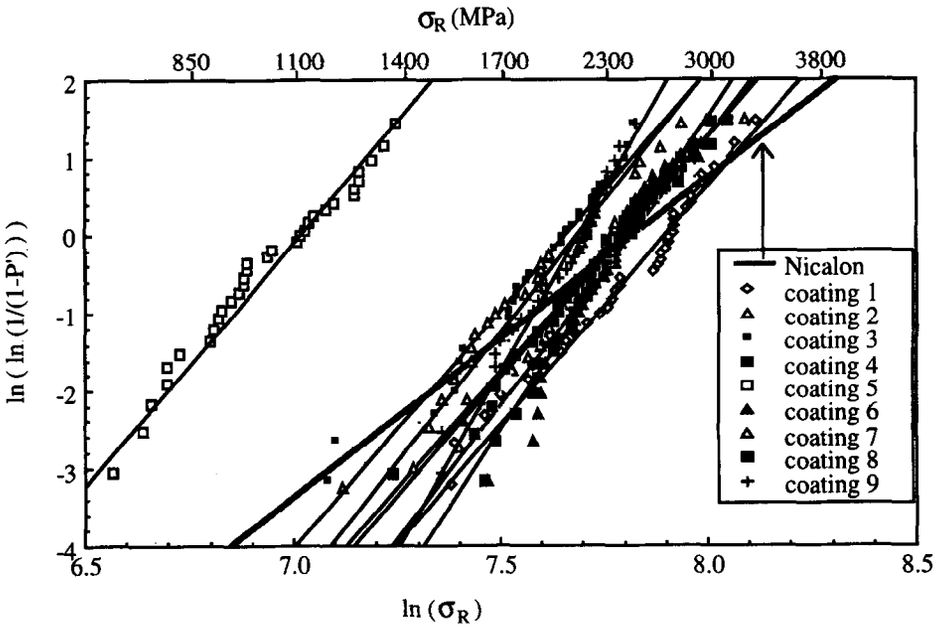

Fig. 12. Weibull plots of the failure stresses of BN coated Nicalon fibers.

small single flat basic structural units (BSUs), (ii) parallel ordering of the BSUs to form distorted columns, (iii) lateral coalescence of the columns to give distorted layers and (iv) with the release of all the defects, the crystal growth may begin and the flat layers form.

By comparison, in a BN coating, the stacks of (002) planes seem to extend preferentially in the lateral direction before ordering parallel between each other. This feature yields few long (002) planes stacked and slightly bent. Further, the parallel ordering of these stacks can be expected to be difficult for boron nitride.

In the conditions 11, the stacking of the (002) planes occurs over longer distances. In the BN coatings processed in the conditions 5, the pinpoint defects are eliminated and the only defects present are in the stacks of the (002) planes (twins, grain boundaries). The step of coalescence of these columns for a perfect graphitization is not achieved, probably related to the low processing temperatures. However, through the XRD spectra and the TEM observation, a three-dimensional order exists in each column, disoriented BN being only present at the grain boundaries.

4.3 Relations between the organization of BN coating and chemical LPCVD kinetics

The structure of the BN-layer is obviously controlled by the LPCVD conditions, in both the deposits on planar substrates and fibres. This progressive organization of the BN structure can be related to a change in chemical deposition mechanism. Indeed, according to Prouhet *et al.*,[21] the chemical rate controlled regime changes as a function of the processing conditions. It was reported that the increase of the temperature and pressure led to a mechanism of deposition involving the major adsorption of $NH_{3(g)}$ on the substrate, followed by the reaction with $BF_{3(g)}$ and the evolution of 3 $HF_{(g)}$. Conversely, with a decrease of the temperature and pressure, the adduct $(BF_3{:}NH_3)_{(g)}$ should be formed in the gaseous phase before its adsorption on the surface to give BN.

The organization of the BN coating can be then expected to be more ordered when the intermediate species is formed at the fibre surface and not in the gaseous phase, i.e. before reaching the substrate surface. Then, if one species (NH_3) is already adsorbed, the second species (BF_3) coming to react has to find a position depending on the free sites around the first species on the substrate surface, i.e. on the already existing (002) planes of the BN layer. This interpretation is in agreement with the major adsorption of NH_3 on the substrate surface. Thus, $BF_{3(g)}$ becomes the rate-limiting species in the kinetics, as experimentally observed.

Similar conclusions were assumed for the CVD of BN from other gaseous phases. When BN is deposited from BCl_3–NH_3–N_2 system, at low pressure, the deposition rate is proportional to the concentration of BCl_3, while it is independent of the concentration of NH_3.[40] The observed relation between the rate-limiting process and the microstructure could be understood by considering the competition between the supply of reactants and the arrangement of atoms on the surface. In the lower temperature region, the formation of the adduct $(BCl_3{:}NH_3)$ in the gaseous phase leads to disordered bonds at the substrate surface, and

to bent layers. On the other hand, in the higher temperature region, supply of reactants is not too fast so that atoms can be regularly arranged to develop hexagonal planes of boron and nitrogen, which form the layer structure at the microscopic scale.

5. Conclusion

At the low temperatures involved in the LPCVD process, the BN coatings are usually almost isotropic. Under such processing conditions, the coated fibres generally have their mechanical properties unchanged, and even increased when the surface defects are healed. The surface coatings are usually rather smooth or exhibit large domes characterizing poorly organized deposits. In more aggressive deposition conditions upon Nicalon fibers, BN interphases are weakly bonded to the fibre surface.

Further, in the domain of CVD conditions, a three-dimensional ordered BN was deposited. Such a coating was identified not as a singularity but as the result of a logic structural evolution with the increase of the four processing parameters involved (pressure, temperature, composition, flow rate). This change in the BN structure was related to different kinetic regimes involved in the LPCVD process. High deposition rate and relatively low supply of BF_3 at the fibre surface seems to favour the deposition of ordered BN coatings.

BN has rarely been processed with a turbostratic texture similar to that of pyrocarbon. From a TEM analysis, the atomic planes within BN coatings tend to display significant bending and to extend preferentially in the lateral direction rather than to lie parallel to each other as columns. In a coating showing a beginning of preferential growth direction, only small zones are well crystallized and seem to correspond to the base of crystals; this order disappears progressively for starting again later in the thickness. In the three-dimensionally ordered BN, large columns form the coating. In each of them, the (002) planes are almost perfectly parallel over distances higher than a micrometre. This coating contains only few percent of carbon and oxygen.

Acknowledgements

This work has been supported by the French Ministry of Education and Research (MRES) and SEP through a grant given to F.R. The authors are grateful to M. Chambon (CUMEMSE) and F. Doux (SEP) for their contributions to TEM observation, as well as to G. Bondieu (SEP) for his help in the processing of BN coatings, to A. Costecalde (SEP), S. Goujard (SEP) and H. Tenailleau (LCTS) for fruitful discussions.

References

1. Evans, A. G. and Marshall, D. B., The mechanical behavior of ceramic matrix composites. *Acta. Metall.*, 1989, **37**, 2567–2583.
2. Quenisset, J. M., Damage mechanisms in composite materials. *23e colloque du groupe français de rhéologie, général conférence* (in French). LMP-CERMUB édition, Bordeaux, 1988, pp. 1–41.
3. Cao, H. C. Bischoff, E., Sbaizero, O., Ruhle, M., Evans, A. G., Marshall, D. B. and Brennan, J. I., Effect of interfaces on the properties of fibre-reinforced ceramics. *J. Am. Ceram. Soc.*, 1990, **73**(6), 1691–1699.
4. Naslain, R., Fibre-matrix interphases and interfaces in ceramic matrix composites processed by CVI. *Composite Interfaces*, 1993, **1**(3), 253–286.
5. Dupel, P., Bobet, J. L., Pailler, R. and Lamon, J., Influence d'interphases pyrocarbone déposées par CVI pulsée sur les caractéristiques mécaniques de matériaux composites unidirectionnels. *J. Phys. III France*, 1995, **5**, 937–951.
6. Lowden, R. A. and More, R. L., The effect of fibre coating on interfacial shear strength and the mechanical behavior of ceramic composites. *Mat. Res. Symp. Proc.*, 1990, **170**, 205–214.
7. Singh, R. N., Role of fibre-matrix interfacial shear stress on the toughness of reinforced oxide matrix composites. *Mat. Res. Symp. Proc.* 1988, **120**, 259–264.
8. Singh, R. N. and Brun, M. R., Effect of boron nitride coating on fibre–matrix interactions. *Ceram. Eng. Sci. Proc.*, 1987, **7** (7–8), 636–643.
9. Singh, R. N., Fibre-matrix interfacial characteristics in a fibre-reinforced ceramics matrix composites. *J. Am. Ceram. Soc.*, **72**(9), 1989, 1764-67.
10. Ricca, N., Composites SiC/cordiérite à interphase BN : élaboration, étude microstructurale et comportement mécanique. Ph.D. Thesis, University of Bordeaux I, 1993.
11. Pease, R. S., Similarities of structure between BN and carbon. *Acta Cryst.*, 1952, **5**, 356–361.
12. Niedenzu, K. and Dawson, J. W., *Boron–nitrogen compounds*. Springer–Verlag, 1965, M. Becke-Goehring, Vol. VI, pp. 147–158.
13. Chrétien, A., Combinaison avec l'azote et le phosphore. In *Traité de chimie minérale*, ed. P. Pascal. Vol. VI. Masson et Cie, Paris, 1961, pp. 249–256.
14. Ingles, T. A. and Popper, P., *Boron Nitride*, ed. A. T. Green. The British Ceramic Research Association, Research Paper No. 398, 1958, pp. 1–27.
15. Ingles, T. A. and Popper, P., *Boron Nitride*, ed. A. T. Green. The British Ceramic Research Association, Research Paper No. 452, 1958, pp. 1–20.
16. Dana, S. S., The properties of low pressure chemical vapor deposited boron nitride thin films. *Mater. Sci. Forum.* 1990, **54 & 55**, 229–260.
17. Rozenberg, A. S., Sinenko, Y. A. and Cherkanov, N. V., Regularities of pyrolytic boron nitride coating formation on a graphite matrix. *J. Mat. Sci.*, 1993, **28**, 5528–5533.
18. Thomas, J., Weston, N. E. and O'Connor, T. E., Turbostratic boron nitride thermal transformation to ordered-layer lattice boron nitride. *J. Am. Chem. Soc.*, 1963, **84**, 4619–4622.
19. Lipp, A., Schwetz, K. A. and Hunold, K., Hexagonal boron nitride : fabrication, properties and applications. *J. European Ceram. Soc.*, 1989, **5**, 3–9.
20. Sugiyama, K. and Itoh, H., Chemical vapor deposition of turbostratic and hexagonal boron nitride. *Mat. Sci. Forum*, 1990, **54 & 55**, 141–152.

21. Prouhet, S., Vignoles, G., Langlais, F., Guette, A. and Naslain, R., On the kinetics of boron nitride CVD from BF_3–NH_3–Ar: 2—Influence of the precursor composition and chemical mechanisms. *European Journal of Solid State and Inorganic Chemistry*, 1993, **T30**, pp. 971–989.
22. Dakye, A. K. Qui, X. and Borek, T., Stability of boron nitride coating on ceramic substrates. *Mat. Res. Soc. Symp. Proc.*, San Francisco, *Better Ceramics Through Chemistry IV*, ed. B. Zelinski, C. Brinker, D. Clark and D. Ulrich, 1990, vol. 180, pp. 807–810.
23. Oda, K. and Yoshio, T., Oxidation kinetics of hexagonal boron nitride powder. *J. Mater. Sci.*, 1993, **28**, 6562–6566.
24. Coffer, C. G. and Economy, J., Oxidation and hydrolytic stability of boron nitride. A new approach to improving the oxidation resistance of carbonaceous structures. *Carbon*, 1995, **33**, 389–395.
25. Hannache, H., Naslain, R. and Bernard, C., Boron nitride chemical vapour infiltration of fibrous materials from BCl_3–NH_3–H_2 or BF_3–NH_3 mixtures : a thermodynamic and experimental approach. *J. Less-Common Met.*, 1983, **95**, 221–246.
26. Pierson, H. D., Boron nitride composites by chemical vapor deposition. *J. Composite Mater.*, 1975, **9**, 228–240.
27. Pasher, D. J., Goretta, K. C., Modder, R. S. and Tressler, R. E., Strengths of ceramics fibers at elevated temperatures. *J. Am. Ceram. Soc.*, 1989, **72**, 284–288.
28. Clark, J. J., Prack, E. R., Maider, M. I. and Sawyer, L. C., Oxidation of SiC ceramic fibre. *Ceram. Eng. Sci. Proc.*, 1986, **7**, 901–913.
29. Labrugère, C., Influence de l'évolution physico-chimique des fibres et de la zone interfaciale fibre/matrice sur le comportement mécanique des composites SiC/C/SiC et SiC/MAS-L après vieillissement thermique sous atmosphère controlée. Ph. D. Thesis No. 998, University of Bordeaux 1, 1993.
30. Dugne, O., Prouhet, S., Guette, A., Naslain, R. and Sevely, J., Interface characterization by transmission electron microscopy and Auger electron spectroscopy in tough SiC-fibre (Nicalon)–SiC matrix composite with a boron nitride interphase. In *Developments in the science and technology of composite materials. Proc. ECCM3*, ed. A. R. Bunsell *et al.* Elsevier Applied Science London and New York, 1989, pp. 129–135.
31. Dugne, O., Prouhet, S., Guette, A., Naslain, R., Fourmeaux, R., Khin, Y., Sevely, J., Rocher, J. P. and Cotteret, J., AES, XPS, and TEM characterization of boron-nitride deposited under chemical vapor infiltration (CVI) conditions. *J. Applied Phys.* 1989, **50** (suppl.), 333–341.
32. Edwards, I. A., In *Introduction to Carbon Science*, ed. H. Marsh. Butterworth & Co., 1989, ch. 1.
33. Oberlin, A., Goma, J. and Rouzaud, J. N., Techniques d'étude des structures et textures (microstructures) des matériaux carbonés. *J. Chimie Physique*, 1984, **81**, 701–710.
34. Permock, G. M. and O'Gara, E., Preparation of carbon fibers sections for light and transmission electron microscopy . *J. Mat. Sci. Letters*, 1990, **9**, 847–849.
35. Rebillat, F., *et al.*, Preparation of cross-sections of coated SiC ex-PCS Nicalon fibers and SiC/SiC microcomposites for TEM observation. To be published.
36. Rebillat, F., Guette, A. and Robin-Brosse, C., Chemical and mechanical alterations of SiC Nicalon fibre properties during the CVD/CVI process of boron nitride. Submitted to *Acta. Metall. and Mater.* (1997).
37. Maya, L., Plasma-enhanced chemical vapor deposition of boron nitride using polymeric cyanoborane as source. *J. Am. Ceram. Soc.*, 1992, **75**, 1985–1987.
38. Economy, J. and Anderson, R. V., Boron nitride fibers. *J. Polym. Sci.*, 1967 No. 19, 283–297.
39. Economy, J. and Lin, R., Boron nitride fibers. In *Boron and Refractory Borides*. Springer-Verlag, Berlin, 1977, pp. 552–564.
40. Tanji, H., Monden, K. and Ide, M., CVD mechanism of pyrolytic boron nitride. *Proc. 10th Int. Conf. on CVD*, ed. G. W. Cullen. The Electrochem. Soc., Pennington, 1987, pp. 562–569.